Chapter 1

InAs Band-Edge Exciton Fine Structure

1.1 Contributions

This work was carried out in collaboration with Oscar Sandoval, a summer student at Lincoln Laboratory. Daniel Harris and Daniel Franke synthesized the nanocrystals. Matt Grein, Ryan Wilson, and Eric Dauler maintained the superconducting detector system used for photoluminescence measurements at Lincoln Laboratory. Greg Steinbrecher constructed the microscope. Thomas Bischof, Igor Coropceanu, and Oscar Sandoval analyzed the data.

1.2 Introduction

Semiconductor nanocrystals rarely, if ever, exhibit emission linewidths which are lifetime-limited. Instead, there are a number of linewidth broadening mechanisms which are relevant under various conditions, such as spectral diffusion,[1,2] charging,[2,3] and excitonic fine structure.[1,3–9] While spectral diffusion and charging are most likely photoinduced effects and thus can be modulated by the excitation rate of the nanocrystals, fine-structure broadening is fundamental to the photophysics of nanocrystals and most likely unavoidable. A complete understanding of the excitonic

energy landscape enables us to determine dephasing rates, linewidths, lifetimes, and other parameters essential to optical applications.

Here we discuss the relationship between the excitonic fine structure and the emission dynamics of InAs/CdS core/shell nanocrystals. At room temperature we find steady-state emission dynamics on order of 150 ns, and as the temperature is lowered we find that the relaxation is greatly slowed (1.9 µs at 3.6 K). We find that these emission dynamics are well-explained by a band-edge model including a pair of "dark" and "bright" excitonic states, separated in energy by 2.3 meV.

1.3 Methods

Nanocrystal cores were prepared following the method reported in Bruns et al.[10]. In this synthesis, 4 mmol indium(III) acetate (1.168 g), 16 mmol myristic acid (3.654 g), and 20 mL 1-octadecene (ODE) were added to a 100 mL round-bottom flask. This solution was heated under vacuum for 2 h. An argon atmosphere was then introduced and the solution was heated to 295 °C. Two injection syringes were prepared, one containing 0.244 mmol tris(trimethylgermyl)arsine[11] ($(TMGe)_3As$, 96 mg) and 4 mL tri-n-octylphosphine (TOP, 4 mL, and the other containing 0.72 mmol $(TMGe)_3As$ (332 mg), 1 mL TOP, and 4 mL ODE. The contents of the first syringe were injected rapidly once the solution had reached 295 °C. After 10 min, the contents of the second syringe were injected at a rate of 5 mL/h. This procedure yielded InAs cores with an absorption peak at 1031 nm, and an emission peak at 1074 nm. Based on existing size calibrations,[12] these cores have an inorganic diameter of 4.9 nm.

To add the epitaxial shell, 5 mL InAs QDs in hexanes (90 nmol 4.9 nm InAs QDs; 100 µmol InAs), 10 mL ODE and 7.5 mL oleylamine were added to a 100 mL round-bottom flask. This solution was degassed at room temperature, then 1 mL of 50 mM $Cd(oleate)_2$ in ODE were added (sufficient for one monolayer). The solution was heated to 100 °C under vacuum, then heated to 240 °C under nitrogen. Two ODE solutions, one containing 45 mM sulfur and the other 50 mM $Cd(oleate)_2$, were injected at a rate of 5 mL/h until 8.2 mL of each solution had been added. This procedure

yielded core/shell InAs/CdS nanocrystals with a 4.9 nm core, a five-monolayer thick shell, a photoluminescence peak at 1170 nm with a FWHM of 210 nm, and an emission quantum yield of 30 %.

To prepare nanocrystal films for optical experiments, we first diluted 1 µL stock InAs/CdS solution with 200 µL toluene and 200 µL PMMA/toluene (2 wt. %). We then deposited 30 µL of this diluted solution onto a 100 µm-thick Z-cut quartz substrate (MTI Corp.), and spun the sample at 5 krpm for 60 s to create a uniform film. This final sample was used without further treatment.

In our microscope, we mounted the sample in a closed-cycle helium cryostat (Montana Instruments, Cryostation). We performed our experiments in an epifluorescence configuration with a 100x near-infrared corrected long working distance objective (Mitutoyo, Plan Apo NIR), using a 640 nm pulsed diode laser for excitation (PicoQuant, LDH-P-C-640B), a 1000 nm short-pass dichroic filter (Thor Labs, DMSP1000), and a 700 nm long-pass emission filter (Thor Labs, FEL0700). The emission was collected into an SMF-28 fiber optic cable using an aspherical lens and directed into a cryostat containing a four-element superconducting nanowire single-photon detecotor (SNSPD), back-illuminated through a silicon substrate.[13–15] The SNSPD elements are read out using a PicoQuant HydraHarp.

1.4 Results

For our sample, we measured the emission lifetime at a variety of temperatures (3.6–295 K), with a laser repetition rate of 100 kHz. We verified the absence of multiexcitonic effects by confirming that the lifetime measured at one excitation power and another measured at a lower power were identical. The low repetition rate was chosen to prevent interpulse excitation at low temperatures, for which the emission lifetime is on the order of 2 µs.

The lifetime of emission at two representative temperatures is shown in Figure 1-1. At 295 K the emission is fit well as a biexponential with time constants of 49 ns and 175 ns. At low temperature the resolution of the fast component seen in Figure 1-1A

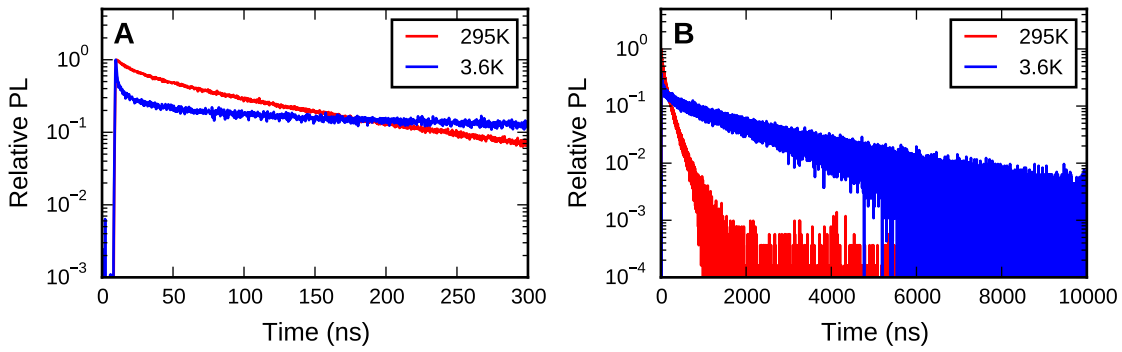

Figure 1-1: Emission lifetime of InAs/CdSe nanocrystals at 3.6 K and 295 K. **A** The emission lifetime of the film at 3.6 K (blue) and 295 K (red). **B** The same data, shown on a longer timescale to demonstrate the 1.9 µs low-temperature lifetime. All data are normalized to the maximum number of counts detected in a histogram bin.

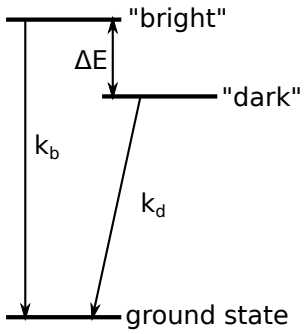

Figure 1-2: The standard three-state band-edge excitonic fine structure model.

is limited by the instrument response function (laser pulse duration ≈ 100 ps, detector jitter ≈ 60 ps), and the remaining signal is fit well as a biexponential (130 ns, 1.9 µs).

Prior reports[4–6,16–18] have suggested that the variability in emission lifetime is to the presence of multiple excitonic fine-structure states. In this model (Figure 1-2), the two lowest-lying excitonic states are a "dark" state, which is spin-forbidden from direct radiation, and a "bright" state, which is spin-allowed. The dark state is lower in energy, on the order of 3 meV for several binary materials.[17] At room temperature both states are approximately equally populated, such that emission primarily occurs through the bright state, but at low temperature only the dark state has significant thermal population. In both cases this manifests as a steady-state emission lifetime defined by the state populations and their relaxation rates (we

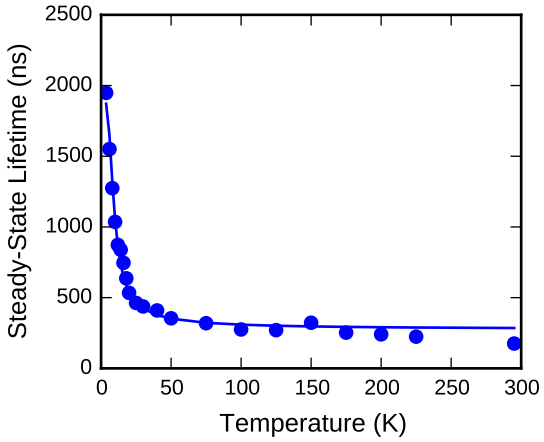

Figure 1-3: The steady-state lifetime of InAs nanocrystal emission as a function of temperature. The solid line is the fit to Equation (1.1).

assume thermal processes are fast relative to exciton recombination):[17]

$$k = f_b k_b + f_d k_d = \frac{k_b e^{-\beta \Delta E} + k_d}{e^{-\beta \Delta E} + 1} \tag{1.1}$$

Fitting this three-parameter model to the temperature-dependent steady-state lifetime, we obtain $k_b = 150\,\text{ns}$, $k_d = 1.9\,\mu\text{s}$, and $\Delta E = 2.3\,\text{meV}$ (Figure 1-3). The bright-state lifetime is comparable to reports on indvidual nanocrystals of comparable size.[15] The energetic splitting is consistent with that measured previously by photoluminescence methods[17] and ultrafast methods,[16] where it was attributed to the confined acoustic phonon energy of the nanocrystal. The agreement between transient oscillatory behavior and an equivalent splitting in state energies led Oron et al.[17] to conclude that all of the materials they studied (CdSe, InAs, PbSe, and CdTe) exhibited the same effective band-edge fine structure, with similar acoustic phonon energies.

These extracted relaxation rates are consistent with the dynamics observed in the PL transient. To fully model the PL transient we introduce the rate $k_{d \leftarrow b}$ for relaxation from the bright state to the dark state (the inverse rate is $k_{d \leftarrow b} e^{-\beta \Delta E}$, to preserve the Boltzmann distribution of population). Estimating this rate to be on the order of 25 ps,[5] we obtain an initial rapid decay consistent with our transient data, the

measurement of which is limited by the finite duration our laser pulse ($\approx 100\,\mathrm{ps}$) and the timing jitter of the detectors ($\approx 60\,\mathrm{ps}$). At intermediate times the kinetic model deviates from the data, but this can be explained by the existence of a distribution of relaxation rates,[5] most readily explained as the result of structural polydispersity of the nanocrystal sample.[15] In principle it is possible to extract an estimate of this distribution from the ensemble data, but a more precise measurement can be achieved by instead measuring the lifetimes of individual molecules.

1.5 Conclusions

We measured the temperature-dependent lifetime of a sample of InAs/CdSe quantum dots, and found that the steady-state relaxation rate is consistent with the excitonic fine-structure model of a bright and dark state coupled by acoustic phonons. We obtain a bright-state lifetime of 150 ns, a dark-state lifetime of 1.9 µs, and a splitting energy of 2.3 meV, which are consistent with previous reports. The relaxation rates and energetic splitting of these states are also consistent with the emission dynamics before the exciton population reaches the steady-state.

1.6 Acknowledgements

This work is sponsored by the Assistant Secretary of Defense for Research & Engineering under Air Force Contract #FA8721-05-C-0002. Opinions, interpretations, conclusions and recommendations are those of the author and are not necessarily endorsed by the United States Government.

Bibliography

[1] Fernée, M. J.; Sinito, C.; Louyer, Y.; Tamarat, P.; Lounis, B. The ultimate limit to the emission linewidth of single nanocrystals. *Nanotechnology* **2013**, *24*, 465703.

[2] Beyler, A. P.; Marshall, L. F.; Cui, J.; Brokmann, X.; Bawendi, M. G. Direct Observation of Rapid Discrete Spectral Dynamics in Single Colloidal CdSe-CdS Core-Shell Quantum Dots. *Phys. Rev. Lett.* **2013**, *111*, 177401.

[3] Fernée, M. J.; Sinito, C.; Louyer, Y.; Potzner, C.; Nguyen, T.-L.; Mulvaney, P.; Tamarat, P.; Lounis, B. Magneto-optical properties of trions in non-blinking charged nanocrystals reveal an acoustic phonon bottleneck. *Nat. Commun.* **2012**, *3*, 1287.

[4] Nirmal, M.; Murray, C. B.; Bawendi, M. G. Fluorescence-line narrowing in CdSe quantum dots: Surface localization of the photogenerated exciton. *Phys. Rev. B* **1994**, *50*, 2293–2300.

[5] Nirmal, M.; Norris, D. J.; Kuno, M.; Bawendi, M. G.; Efros, Al. L.; Rosen, M. Observation of the "Dark Exciton" in CdSe Quantum Dots. *Phys. Rev. Lett.* **1995**, *75*, 3728–3731.

[6] Liu, H.; Guyot-Sionnest, P. Photoluminescence Lifetime of Lead Selenide Colloidal Quantum Dots. *J. Phys. Chem. C* **2010**, *114*, 14860–14863.

[7] Fernée, M. J.; Louyer, Y.; Tamarat, P.; Lounis, B. Comment on "Spin-Flip Limited Exciton Dephasing in CdSe/ZnS Colloidal Quantum Dots". *Phys. Rev. Lett.* **2012**, *109*, 229701.

[8] Sinito, C.; Fernée, M. J.; Goupalov, S. V.; Mulvaney, P.; Tamarat, P.; Lounis, B. Tailoring the Exciton Fine Structure of Cadmium Selenide Nanocrystals with Shape Anisotropy and Magnetic Field. *ACS Nano* **2014**, *8*, 11651–11656.

[9] Fernée, M. J.; Tamarat, P.; Lounis, B. Spectroscopy of single nanocrystals. *Chem. Soc. Rev.* **2014**, *43*, 1311–1337.

[10] Bruns, O. T.; Bischof, T. S.; Harris, D. K.; Shi, Y.; Riedemann, L.; Reiberger, T.; Bartelt, A.; Jaworski, F. B.; Franke, D.; Wilson, M. W.; Chen, O.; Wei, H.;

Hwang, G. W.; Montana, D.; Coropceanu, I.; Kloepper, J.; Heeren, J.; Fukumura, D.; Jensen, K. F.; Jain, R. K.; Bawendi, M. G. Next generation *in vivo* optical imaging with short-wave infrared quantum dots. *Submitted*

[11] Harris, D. K.; Bawendi, M. G. Improved Precursor Chemistry for the Synthesis of III–V Quantum Dots. *J. Am. Chem. Soc.* **2012**, *134*, 20211–20213.

[12] Yu, P.; Beard, M. C.; Ellingson, R. J.; Ferrere, S.; Curtis, C.; Drexler, J.; Luiszer, F.; Nozik, A. J. Absorption Cross-Section and Related Optical Properties of Colloidal InAs Quantum Dots. *J. Phys. Chem. B* **2005**, *109*, 7084–7087.

[13] Dauler, E. A.; Kerman, A. J.; Robinson, B. S.; Yang, J. K.; Voronov, B.; Goltsman, G.; Hamilton, S. A.; Berggren, K. K. Photon-number-resolution with sub-30-ps timing using multi-element superconducting nanowire single photon detectors. *J. Mod. Opt.* **2009**, *56*, 364–373.

[14] Correa, R. E.; Dauler, E. A.; Nair, G.; Pan, S. H.; Rosenberg, D.; Kerman, A. J.; Molnar, R. J.; Hu, X.; Marsili, F.; Anant, V.; Berggren, K. K.; Bawendi, M. G. Single Photon Counting from Individual Nanocrystals in the Infrared. *Nano Lett.* **2012**, *12*, 2953–2958.

[15] Bischof, T. S.; Correa, R. E.; Rosenberg, D.; Dauler, E. A.; Bawendi, M. G. Measurement of Emission Lifetime Dynamics and Biexciton Emission Quantum Yield of Individual InAs Colloidal Nanocrystals. *Nano Lett.* **2014**, *14*, 6787–6791.

[16] Cerullo, G.; De Silvestri, S.; Banin, U. Size-dependent dynamics of coherent acoustic phonons in nanocrystal quantum dots. *Phys. Rev. B* **1999**, *60*, 1928–1932.

[17] Oron, D.; Aharoni, A.; de Mello Donega, C.; van Rijssel, J.; Meijerink, A.; Banin, U. Universal Role of Discrete Acoustic Phonons in the Low-Temperature Optical Emission of Colloidal Quantum Dots. *Phys. Rev. Lett.* **2009**, *102*, 177402.

[18] Robel, I.; Shabaev, A.; Lee, D. C.; Schaller, R. D.; Pietryga, J. M.; Crooker, S. A.; L. Efros, A.; Klimov, V. I. Temperature and Magnetic-Field Dependence of Radiative Decay in Colloidal Germanium Quantum Dots. *Nano Lett.* **2015**, *15*, 2685–2692.